

Advantage of using QUICKEST scheme for the approximation of the transport operator in the equations of motion in the ocean circulation model

D.F. Yusupova

Abstract. This paper presents a study aimed at improving numerical models of the ocean dynamics. We evaluate the sensitivity of the regional ocean circulation model to the numerical schemes used to approximate the transport operator in the equations of motion; we investigate the influence of the numerical scheme on the flow field, reproduced by the numerical model. Numerical experiments involving two versions of the numerical circulation model were conducted for the basin, which includes the Arctic Ocean and the North Atlantic. A comparative analysis of the experimental results has shown that the rejection of a generally used central difference scheme for the equations of motion and the use of a scheme of higher order accuracy QUICKEST [1] conduce to the reproduction of more intense currents responsible for the exchange of water between the oceans. Even in models with a coarse spatial resolution on the numerical grid, where nonlinear effects do not have a significant impact on the structure of model fields, there are differences between the obtained model fields. The use of more accurate schemes for approximation of the transport process in the equations of motion make possible to reduce the viscosity coefficients and to obtain a smoother flow pattern, whose intensity is increased.

1. Introduction

The modeling of advective transport is one of the most important Ocean Process computational modeling problems. At the end of the 1960's Bryan's publication [2] appeared, where the full nonlinear ocean dynamic model was presented, which initiates an intensive ocean circulation research by means of numerical modeling. This model [2] used spatial central difference schemes for advection operators. In the sequel, the problem was repeatedly discussed in that the central difference scheme has a numerical dispersion causing oscillations in numerical solutions. To suppress these oscillations, it is necessary to use high-diffusion significantly coefficients, exceeding physical values and, hence, smoothing fronts and currents. The use of first order upwind difference schemes in some models caused a scheme viscosity also smoothing a numerical solution. At the beginning of the 1990's an intensive research into tracer advection numerical schemes began aimed at their use in the ocean dynamic models for the temperature and salinity calculation [3–5].

The numerical schemes with a reduced scheme viscosity that are a combination of the central difference and the upwind-difference schemes [6], were

coming into use. In [7], the scheme viscosity was excluded by means of the Richardson extrapolation.

The authors of [4, 5] indicated to the fact that the use of the FCT, the QUICK schemes allows one to obtain a hydrological fields distribution free from numerical oscillations and to significantly improve the ocean process definition in comparison with the central difference scheme. Currently, it remains a highly topical problem [8, 9]. In [10] it was demonstrated that substitution of a scheme with a reduced scheme viscosity by the QUICKEST scheme [1] in the equations of temperature and salinity advection allows one in the context of rather a rough resolution to describe the Atlantic water spreading in the Arctic Ocean.

At the same time, in any ocean circulation numerical model, the central difference schemes for the advection operator are still used in the moment advection equations. An extended analysis of the moment advection equations shows that the primary balance in the ocean is struck between the Coriolis force and the pressure gradients. Close to the side boundaries, the surface and bottom viscous term has an essential impact.

Nonlinear effects in the velocity field are revealed only in high-resolution models. Therefore numerical schemes, used for approximation of the momentum advection equation, generally have second or a lower order of accuracy. The progressively improving computer engineering allows us gradually to go on to the problems, where nonlinear processes are of paramount importance. Therefore the ocean dynamic numerical models must be developed for improving the advection description in a flow field.

The present paper is a sequel to study [10]. Numerical experiments are made for the Arctic—North-Atlantic basin. In current studies of the Earth's climate changing the Arctic—North-Atlantic interaction is of primary concern. Many international projects are aimed at investigation these regions processes, field study data processing, and development of the ocean dynamic numerical models. AOMIP (The Arctic Ocean Intercomparison Project, http://fish.cims.nyu.edu/project_aomip/overview.html) is one of these projects. Its object is a comparison of the ocean-ice interaction numerical models and causation of the qualitative and the quantitative distinctions in numerical experiments results for the development of new standard models, enabling the reproducing of climate changing.

In the present paper, the problem of the influence of an advection numerical scheme in the momentum equation on the flow field reproduced by a numerical model is investigated. For a set of momentum equations, two schemes are examined: the central difference scheme and the QUICKEST scheme. Let us testify that even in models with a rough resolution, where nonlinear effects have no significant impact on the model fields structure, there are differences between the derived model fields. The use of more accurate schemes for approximation of the transport process in the equations of

motion allow us to reduce the viscosity coefficients and to obtain a smoother flow pattern, whose intensity is increased.

2. The ocean circulation model

2.1. The modeling domain. To simulate the processes of interaction between the Arctic Basin and the North Atlantic, we considered the region of the Arctic Ocean and the North Atlantic, starting with 20° S. The numerical grid is a union of 1° × 1° grid in the spherical coordinate system for the North Atlantic and a reprojective grid with a finer resolution of the Arctic Ocean [11]. A maximum resolution in the polar regions is equal to 35 km. On average, the nodes of the numerical grid in the area of the Arctic Ocean are at a distance of about 50 km. The vertical partitioning represents 33 horizontal levels with concentration at the surface, where the resolution is 10 m.

2.2. The numerical model. The numerical model used for investigation, is a regional ocean model developed at the ICMMG SB RAS. The history of the model originates from the large-scale ocean model [12,13]. A description of the latest version of the model was presented in papers [10,14].

In the system of orthogonal curvilinear coordinates, the full nonlinear hydrothermodynamic equations of the ocean are considered using conventional approximations: Boussinesq, hydrostatics and “solid lid”.

The system includes the equation for the horizontal velocity components:

$$\begin{aligned} \frac{\partial u}{\partial t} + L(u) - Kuv - fv &= -\frac{1}{\rho_0 h_x} \frac{\partial p}{\partial x} + \frac{\partial}{\partial z} \nu \frac{\partial u}{\partial z} + F(u, \mu), \\ \frac{\partial v}{\partial t} + L(v) - Ku^2 + fu &= -\frac{1}{\rho_0 h_y} \frac{\partial p}{\partial y} + \frac{\partial}{\partial z} \nu \frac{\partial v}{\partial z} + F(v, \mu), \end{aligned} \quad (1)$$

here

$$L(\xi) = \frac{1}{h_x h_y} \left[\frac{\partial}{\partial x} (h_y u \xi) + \frac{\partial}{\partial y} (h_x v \xi) \right] + \frac{\partial}{\partial z} (w \xi), \quad (2)$$

$$F(\xi, \mu) = \frac{1}{h_x h_y} \left[\frac{\partial}{\partial x} \left(\mu \frac{h_y}{h_x} \frac{\partial \xi}{\partial x} \right) + \frac{\partial}{\partial y} \left(\mu \frac{h_x}{h_y} \frac{\partial \xi}{\partial y} \right) \right], \quad (3)$$

the continuity equation

$$\frac{1}{h_x h_y} \left[\frac{\partial}{\partial x} (h_y u) + \frac{\partial}{\partial y} (h_x v) \right] + \frac{\partial w}{\partial z} = 0, \quad (4)$$

the hydrostatic equation

$$\frac{\partial \rho}{\partial z} = -\rho g, \quad (5)$$

the equation of state

$$\rho = \rho(T, S, p), \quad (6)$$

the transport-diffusion equation for heat and salt

$$\begin{aligned}\frac{\partial T}{\partial t} + L(T) &= \frac{\partial}{\partial z} \nu_T \frac{\partial T}{\partial z} + F(T, \mu_T), \\ \frac{\partial S}{\partial t} + L(S) &= \frac{\partial}{\partial z} \nu_S \frac{\partial S}{\partial z} + F(S, \mu_S),\end{aligned}\tag{7}$$

where we use the following notations: z is the vertical coordinate with a positive direction from the surface to the center of the Earth, u, v are the horizontal velocity components, T is potential temperature ($^{\circ}\text{C}$), S is salinity ($\%$), ρ is density of water, $\rho_0 = \text{const}$ is a standard density, p is pressure, $f = 2\Omega \sin \varphi$ is the Coriolis parameter, φ is latitude, μ, ν and $\mu_{T,S}, \nu_{T,S}$ are the coefficients of horizontal and vertical viscosity and diffusion, and h_x, h_y are metric coefficients.

Boundary conditions for the original system are the following:

- on the surface $z = 0$:

$$w = 0, \quad \nu \frac{\partial \mathbf{U}}{\partial z} = -\frac{\boldsymbol{\tau}}{\rho_0}, \quad \frac{\partial(T, S)}{\partial z} = (Q_T, Q_S),\tag{8}$$

- on the bottom $z = H$:

$$w = \mathbf{U} \cdot \nabla H, \quad \nu \frac{\partial \mathbf{U}}{\partial z} = -R(u^2 + v^2)^{1/2} \mathbf{U}, \quad \frac{\partial(T, S)}{\partial z} = 0,\tag{9}$$

- on the lateral boundaries Γ_0 :

$$\frac{\partial \mathbf{U} \cdot \mathbf{l}}{\partial n} = 0, \quad \mathbf{U} \cdot \mathbf{n} = 0, \quad \frac{\partial(T, S)}{\partial n} = 0.\tag{10}$$

Here $\boldsymbol{\tau}$ is vector of the wind stress, $\mathbf{U} = (u, v)$ is vector of horizontal velocity components on the corresponding horizontal coordinates, R is a friction coefficient on the bottom, \mathbf{l}, \mathbf{n} are the tangential and thenormal unit vectors to the contour of the boundary Γ , respectively, and Q_T, Q_S are fluxes of heat and salt on the surface.

2.3. A modification of the model. A modification of the numerical model, provided in this paper, concerns the calculation of the horizontal velocity components. In the previous version of the numerical model [10,14], further denoted as M1, the system of transport–diffusion equations

$$\begin{aligned}\frac{\partial u}{\partial t} + L(u) &= \frac{\partial}{\partial z} \nu \frac{\partial u}{\partial z} + \mu \Delta u, \\ \frac{\partial v}{\partial t} + L(v) &= \frac{\partial}{\partial z} \nu \frac{\partial v}{\partial z} + \mu \Delta v\end{aligned}\tag{11}$$

is solved using the method of splitting a 3D operator by spatial variables. In 1D equations for the approximation of the transport operator, the central difference scheme is used. For the time approximation, an implicit scheme is used. In a modified version of the model, further denoted as M2, system of equations (11) is solved in two stages:

$$\frac{\partial u}{\partial t} + L(u) = 0, \quad \frac{\partial v}{\partial t} + L(v) = 0, \quad (12)$$

$$\frac{\partial u}{\partial t} = \frac{\partial}{\partial z} \nu \frac{\partial u}{\partial z} + \mu \Delta u, \quad \frac{\partial v}{\partial t} = \frac{\partial}{\partial z} \nu \frac{\partial v}{\partial z} + \mu \Delta v. \quad (13)$$

Diffusion part (13) is realized using the splitting on 1D operators and a subsequent solution using the implicit schemes in time.

To approximate system of transport equations (12), QUICKEST-scheme with respect to [1] is used. According to results of conducted preliminary tests with the schemes QUICKEST, UTOPIA [15], SOM [16], the QUICKEST-scheme is a reasonable compromise between the efficiency and the cost calculations. The efficiency of this scheme for the transport equation of heat and salt in the model M1 is described in [10].

In model M2, the QUICKEST-scheme is implemented as follows:

$$u_{i,j}^{n+1} = u_{i,j}^n - (M_e u_e - M_w u_w) - (M_n u_n - M_s u_s) - (M_d u_d - M_p u_p), \quad (14)$$

where

$$\begin{aligned} u_e &= \frac{u_{i,j,k}^n + u_{i+1,j,k}^n}{2} - M_e \frac{\Delta x_i}{2} \nabla_e - \frac{\Delta x_i^2}{6} (1 - M_e^2) \varkappa_e, \\ u_w &= \frac{u_{i,j,k}^n + u_{i-1,j,k}^n}{2} - M_w \frac{\Delta x_{i-1,j,k}}{2} \nabla_w - \frac{\Delta x_{i-1,j,k}^2}{6} (1 - M_w^2) \varkappa_w, \\ u_n &= \frac{u_{i,j,k}^n + u_{i,j+1,k}^n}{2} - M_n \frac{\Delta y_{i,j,k}}{2} \nabla_n - \frac{\Delta y_{i,j,k}^2}{6} (1 - M_n^2) \varkappa_n, \\ u_s &= \frac{u_{i,j,k}^n + u_{i,j-1,k}^n}{2} - M_s \frac{\Delta y_{i,j-1,k}}{2} \nabla_s - \frac{\Delta y_{i,j-1,k}^2}{6} (1 - M_s^2) \varkappa_s, \\ u_d &= \frac{u_{i,j,k}^n + u_{i,j,k+1}^n}{2} - M_d \frac{\Delta z_{i,j,k}}{2} \nabla_d - \frac{\Delta z_{i,j,k}^2}{6} (1 - M_d^2) \varkappa_d, \\ u_p &= \frac{u_{i,j,k}^n + u_{i,j,k-1}^n}{2} - M_p \frac{\Delta z_{i,j,k-1}}{2} \nabla_p - \frac{\Delta z_{i,j,k-1}^2}{6} (1 - M_p^2) \varkappa_p; \end{aligned}$$

$$\begin{aligned} M_e &= \frac{(u_{i+1,j,k} + u_{i,j,k}) \Delta t}{\Delta x_{i,j,k}}, & \nabla_e &= \frac{u_{i+1,j,k} - u_{i,j,k}}{\Delta x_{i,j,k}}, \\ M_w &= \frac{(u_{i,j,k} + u_{i-1,j,k}) \Delta t}{\Delta x_{i,j-1,k}}, & \nabla_w &= \frac{u_{i,j,k} - u_{i-1,j,k}}{\Delta x_{i-1,j,k}}, \end{aligned}$$

$$\begin{aligned}
M_n &= \frac{(v_{i,j+1,k} + v_{i,j,k})\Delta t}{\Delta y_{i,j,k}}, & \nabla_n &= \frac{u_{i,j+1,k} - u_{i,j,k}}{\Delta y_{i,j,k}}, \\
M_s &= \frac{(v_{i,j,k} + v_{i,j-1,k})\Delta t}{\Delta y_{i,j-1,k}}, & \nabla_s &= \frac{u_{i,j,k} - u_{i,j-1,k}}{\Delta y_{i,j-1,k}}, \\
M_d &= \frac{(w_{i,j,k+1} + w_{i,j,k})\Delta t}{\Delta z_{i,j,k}}, & \nabla_d &= \frac{u_{i,j,k+1} - u_{i,j,k}}{\Delta z_{i,j,k}}, \\
M_p &= \frac{(w_{i,j,k} + w_{i,j,k-1})\Delta t}{\Delta z_{i,j,k-1}}, & \nabla_p &= \frac{u_{i,j,k} - u_{i,j,k-1}}{\Delta z_{i,j,k-1}}.
\end{aligned}$$

The value of the curvature \varkappa (second derivative) depends on the direction of flow:

$$\begin{aligned}
\varkappa_e &= \begin{cases} \frac{2}{\Delta x_{i,j,k} + \Delta x_{i-1,j,k}} \left(\frac{u_{i+1,j,k} - u_{i,j,k}}{\Delta x_{i,j,k}} - \frac{u_{i,j,k} - u_{i-1,j,k}}{\Delta x_{i-1,j,k}} \right), & u > 0, \\ \frac{2}{\Delta x_{i+1,j,k} + \Delta x_{i,j,k}} \left(\frac{u_{i+2,j,k} - u_{i+1,j,k}}{\Delta x_{i+1,j,k}} - \frac{u_{i+1,j,k} - u_{i,j,k}}{\Delta x_{i,j,k}} \right), & u < 0; \end{cases} \\
\varkappa_w &= \begin{cases} \frac{2}{\Delta x_{i-1,j,k} + \Delta x_{i-2,j,k}} \left(\frac{u_{i,j,k} - u_{i-1,j,k}}{\Delta x_{i-1,j,k}} - \frac{u_{i-1,j,k} - u_{i-2,j,k}}{\Delta x_{i-2,j,k}} \right), & u > 0, \\ \frac{2}{\Delta x_{i,j,k} + \Delta x_{i-1,j,k}} \left(\frac{u_{i+1,j,k} - u_{i,j,k}}{\Delta x_{i,j,k}} - \frac{u_{i,j,k} - u_{i-1,j,k}}{\Delta x_{i-1,j,k}} \right), & u < 0; \end{cases} \\
\varkappa_n &= \begin{cases} \frac{2}{\Delta y_{i,j,k} + \Delta y_{i,j-1,k}} \left(\frac{u_{i,j+1,k} - u_{i,j,k}}{\Delta y_{i,j,k}} - \frac{u_{i,j,k} - u_{i,j-1,k}}{\Delta y_{i,j-1,k}} \right), & v > 0, \\ \frac{2}{\Delta y_{i,j+1,k} + \Delta y_{i,j,k}} \left(\frac{u_{i,j+2,k} - u_{i,j+1,k}}{\Delta y_{i,j+1,k}} - \frac{u_{i,j+1,k} - u_{i,j,k}}{\Delta y_{i,j,k}} \right), & v < 0; \end{cases} \\
\varkappa_s &= \begin{cases} \frac{2}{\Delta y_{i,j-1,k} + \Delta y_{i,j-2,k}} \left(\frac{u_{i,j,k} - u_{i,j-1,k}}{\Delta y_{i,j-1,k}} - \frac{u_{i,j-1,k} - u_{i,j-2,k}}{\Delta y_{i,j-2,k}} \right), & v > 0, \\ \frac{2}{\Delta y_{i,j,k} + \Delta y_{i,j-1,k}} \left(\frac{u_{i,j+1,k} - u_{i,j,k}}{\Delta y_{i,j,k}} - \frac{u_{i,j,k} - u_{i,j-1,k}}{\Delta y_{i,j-1,k}} \right), & v < 0; \end{cases} \\
\varkappa_d &= \begin{cases} \frac{2}{\Delta z_{i,j,k} + \Delta z_{i,j,k-1}} \left(\frac{u_{i,j,k+1} - u_{i,j,k}}{\Delta z_{i,j,k}} - \frac{u_{i,j,k} - u_{i,j,k-1}}{\Delta z_{i,j,k-1}} \right), & w > 0, \\ \frac{2}{\Delta z_{i,j,k+1} + \Delta z_{i,j,k}} \left(\frac{u_{i,j,k+2} - u_{i,j,k+1}}{\Delta z_{i,j,k+1}} - \frac{u_{i,j,k+1} - u_{i,j,k}}{\Delta z_{i,j,k}} \right), & w < 0; \end{cases} \\
\varkappa_p &= \begin{cases} \frac{2}{\Delta z_{i,j,k-1} + \Delta z_{i,j,k-2}} \left(\frac{u_{i,j,k} - u_{i,j,k-1}}{\Delta z_{i,j,k-1}} - \frac{u_{i,j,k-1} - u_{i,j,k-2}}{\Delta z_{i,j,k-2}} \right), & w > 0, \\ \frac{2}{\Delta z_{i,j,k} + \Delta z_{i,j,k-1}} \left(\frac{u_{i,j,k+1} - u_{i,j,k}}{\Delta z_{i,j,k}} - \frac{u_{i,j,k} - u_{i,j,k-1}}{\Delta z_{i,j,k-1}} \right), & w < 0. \end{cases}
\end{aligned}$$

Approximation of the equation for v -components of velocity is similarly done.

3. Numerical experiments

In the numerical experiments, an array of climatic Data PHC [17] was used as the initial data for temperature and salinity. The absolute water temperature represented in the data, was re-counted for a potential temperature distribution. Velocities were set equal to zero.

A sequence of numerical experiments can be divided into two phases.

At the first stage, we carry out the calculation of a quasi-stationary state of the ocean to simulate a system of currents of the Arctic Ocean and the North Atlantic.

Testing the model was carried out with no ice cover at a fixed seasonal course of constraining forces at the ocean surface for 5 years of model time. The lack of ice in the model was offset by “restoring” condition (cf. [18]) of the estimated temperature T and the salinity S on the surface of the ocean to the climatic distribution values [19,20] by the formulas

$$k \frac{\partial T}{\partial z} = \gamma_T (T - T^*), \quad k \frac{\partial S}{\partial z} = \gamma_S (S - S^*), \quad (15)$$

where T^* , S^* are climatic data, γ is a “restoring” parameter, equal to 5 days.

To calculate the momentum flux, an array of data of the wind shear stress was used [21]. The lateral border for this experiment was considered to be closed. Using the “restoring” condition to the salinity of the ocean surface provided in the surface layer of the presence of fresh water from rivers. At the second stage, we used the wind field obtained with the archive data NCEP / NCAR [22] for the period from 1948 to 1973.

The estimation of the diffusion coefficient necessary for the suppression of oscillations in the numerical solution of the transport-diffusion equation for models, using the central difference scheme, presented in [23] based on the stationary equation solution of the form:

$$U \frac{\partial \varphi}{\partial x} = \mu \frac{\partial^2 \varphi}{\partial x^2}. \quad (16)$$

The choice of the numerical solutions in the form of $\varphi_i = a + b\xi^i$ results in the condition $U\Delta x/\mu < 2$, which ensures non-negative ξ and, hence, the absence of oscillations in the numerical solution.

Assuming that the characteristic scale of velocity in the temperate latitudes in the model is equal to 10 cm/s, and the grid size of ~ 100 km, we find that the value of viscosity, sufficient to suppress the oscillations is equal to $5 \cdot 10^7$ cm²/s.

For the Arctic region, the grid size is, on average, equal to 50 km, the characteristic velocity of order 2 cm/s, which corresponds to the viscosity of $5 \cdot 10^6$ cm²/s. These values can be reduced on the assumption of a smooth

behavior of the solution that is checked for each model in the numerical experiment.

The scheme QUICKEST is a numerical scheme of third order accuracy, although not monotonic. However, the numerical solution obtained for 1D transport equation, shows a distinct advantage of the QUICKEST scheme as compared to the scheme. Presentation of the numerical solution in the form $T_j^n = \text{Re}[\exp(ijk\Delta x)]$, $|T^{n+1}| = |\lambda||T^n|$, where i is an imaginary unit, k is wavenumber, allows building a dependence λ^2 from $k\Delta x$ for different values of the Courant number c . From the analysis it follows that QUICKEST is stable when the Courant number $c \leq 1$.

It effectively suppresses the short-wave and leaves the transition factor close to unity for long waves [10]. This allows us to reduce the value of the required viscosity.

Numerical experiments were conducted with the following model parameters (cm^2/s):

	Model M1	Model M2
In the polar latitudes	10^6	10^6
In the temperate latitudes	10^7	10^6
At the equator	$5 \cdot 10^8$	$5 \cdot 10^8$

4. Results of numerical experiments

A flow field, obtained at the first stage reflects the picture of North Atlantic water circulation (Figure 1) and, also, the water exchange between the oceans. The model results represent subtropical anticyclonic North Atlantic circulation with most intensive flow Gulfstream and its continuation North Atlantic flow; subpolar cyclonic circulation, in whose east part the North Atlantic flow water is transported to the north. In the Arctic basin (Figure 3) the following flows are displayed: the Norwegian flow, transporting the warm Atlantic water northward, the East Greenlandic flow, transporting the cold arctic water southward, anticyclonic circulation of the Canadian basin and cyclonic circulation of the Atlantic water in the Arctic.

Results of the numerical experiment matching for two versions of the model have shown that more intensive flows were obtained in Model M2 in comparison with the results of Model M1. A flow intension increase in the upper layer of the ocean can be observed through the vertical section in the primary current, which are responsible for the Arctic—North Atlantic water exchange: the North Atlantic (Figure 2), the East Greenlandic and the Norwegian flows (Figures 4). The results revealed that the velocity of the basin primary currents increased at the account of model modification: the North Atlantic flow—8 cm/s for 1 and 12 cm/s for 2; the East Greenlandic flow—4 cm/s for 1 and 8 cm/s for 2; Norwegian flow—4 cm/s for 1 and 9 cm/s for 2.

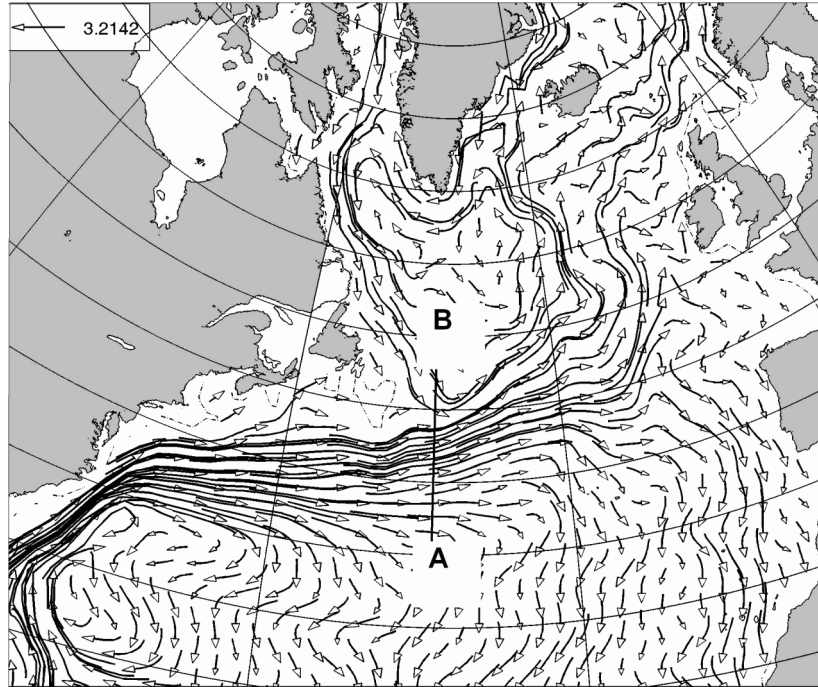


Figure 1. Field of calculated currents in the North Atlantic at a depth of 100 m

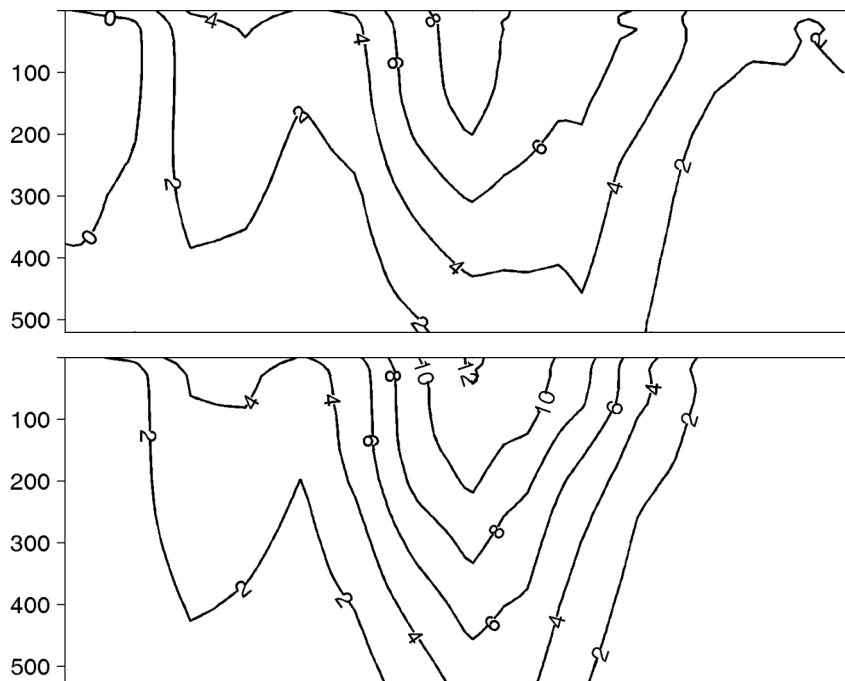


Figure 2. Flow field in the vertical section AB for M1 (top) and M2 (bottom)

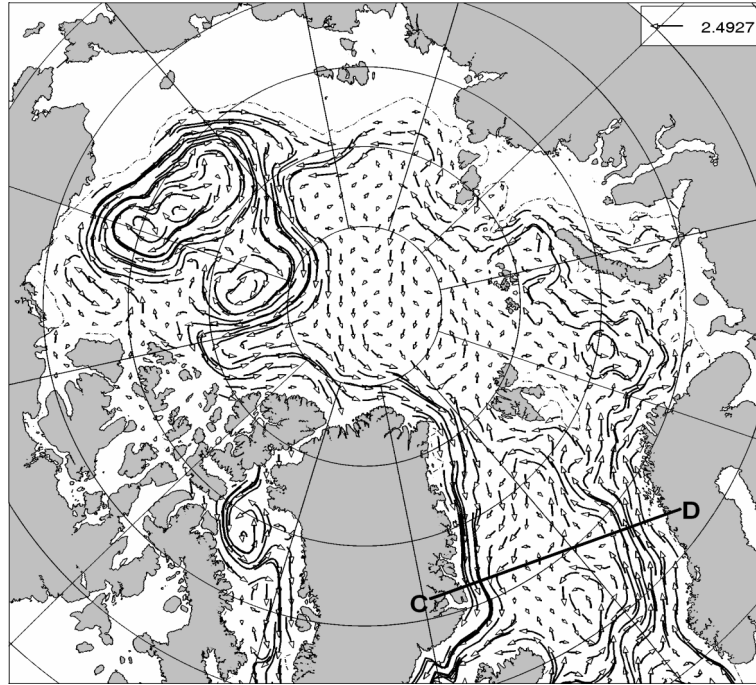


Figure 3. Field of calculated currents in the Arctic at a depth of 100m

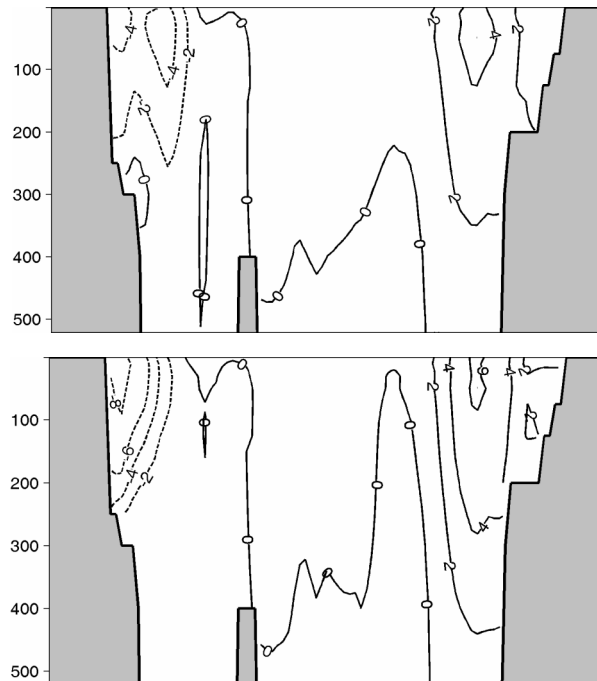


Figure 4. Flow field in the vertical section CD for M1 (top) and M2 (bottom)

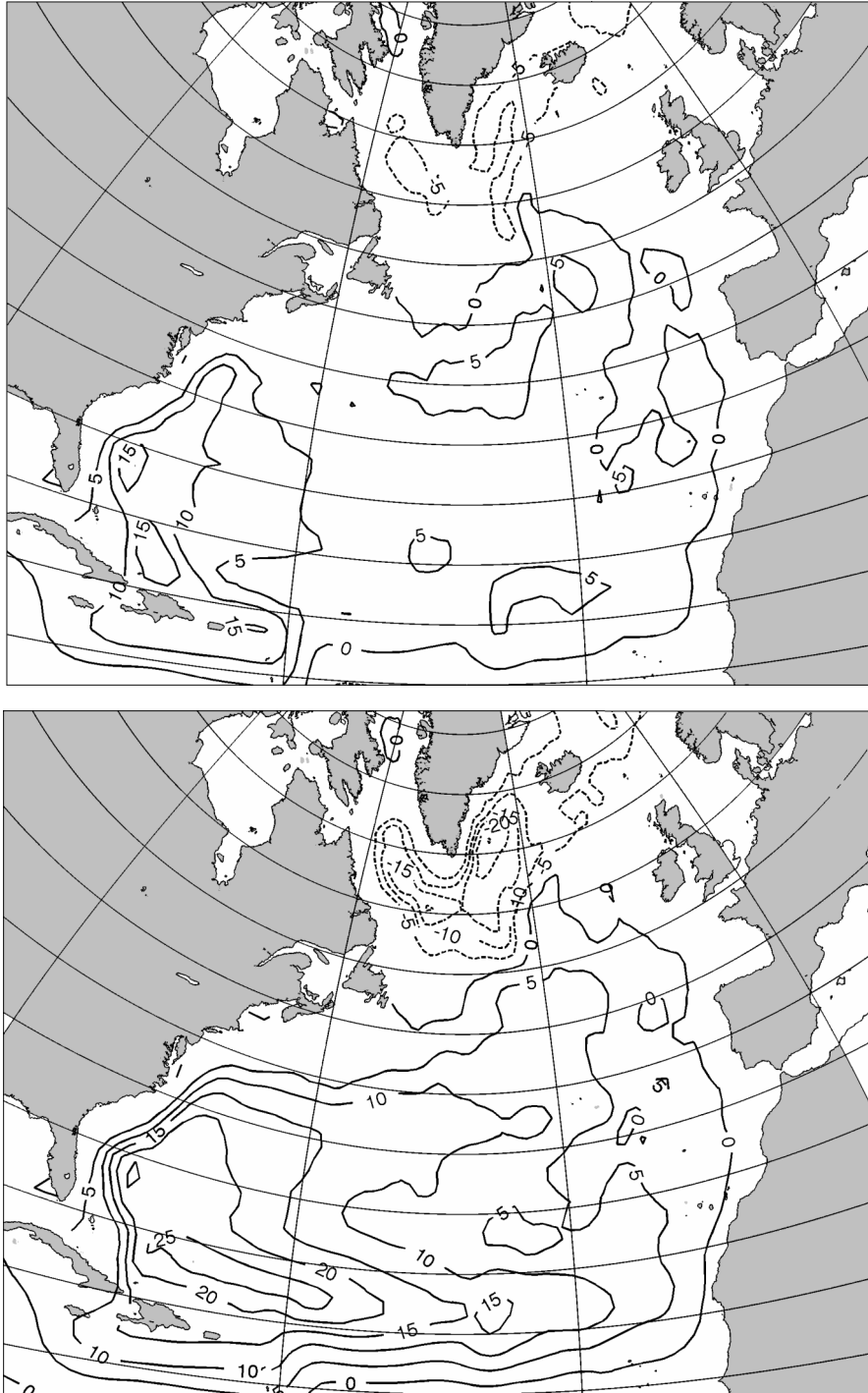


Figure 5. Distribution of the integral values of the stream function in 1973 for M1 (top) and M2 (bottom)

The second numerical experiment was conducted for the time interval from 1948 to 1973. The distribution of the wind field for this period reflects the situation of the negative phase of the North Atlantic Oscillation [24] in the atmosphere, which brings about a weakening of the major large-scale circulations in the North Atlantic, the lower flux of the warm Atlantic waters in the Arctic. In numerical models, where the currents are usually obtained underestimated, the modeling of the water exchange in this period represents certain difficulties. The difference in the results of numerical experiments obtained from Models M1 and M2 is most obvious from the picture of vertically-averaged integral circulation of the ocean, whose distribution in 1973 is presented in Figure 5. From these pictures, it follows that despite the overall deformation of the subtropical gyre in the North Atlantic and weakening of the circulation, in Model M2 subpolar front is more pronounced. A more intensive and subpolar circulation cell is derived from calculations of M2. In the Arctic, differences between the experiments are less pronounced, but it should be noted that as a result of applying the scheme QUICKEST we obtained a smoother distribution of flow fields in the areas with complex bottom topography.

5. Conclusion

In the present study, we evaluate the sensitivity of the regional ocean circulation model to the numerical schemes used to approximate the transport operator in the equations of motion.

It is shown that the rejection of the central difference scheme traditionally used for the equations of motion and the use of a scheme of higher order accuracy QUICKEST, conduce to the reproduction of more intense currents responsible for the exchange of water between the oceans.

In this case, this process is clearly expressed even for a model on a one-degree grid. It is assumed that with the use of a finer mesh, with more expressed nonlinear processes, the advantages of the scheme QUICKEST will be even more noticeable.

References

- [1] Leonard B.P. Elliptic systems: Finite-difference method IV / W.J. Minkowycz, E.M. Sparrow, G.E. Schneider, R.H. Pletcher, ed. // Handbook of Numerical Heat Transfer. — New York: Wiley, 1988. — P. 347-378.
- [2] Bryan K. A numerical method for the study of the circulation of the world ocean // J. Comput. Phys. — 1969. — Vol. 4. — P. 347-376.
- [3] Hasumi H., Sugimoto N. Sensitivity of a global ocean general circulation model to tracer advection schemes // J. Phys. Oceanogr. — 1999. — Vol. 29. — P. 2730-2740.

-
- [4] Holland W.R., Chow J.C., Bryan F.O. Application of a third-order upwind scheme in the NCAR ocean model // *J. Climate*.—1998.—Vol. 11.—P. 1487–1493.
- [5] Gerdes R., Köberle C., Willebrand J. The influence of numerical advection schemes on the results of ocean general circulation models // *Climate Dyn.*—1991.—Vol. 5.—P. 211–226.
- [6] Maier-Reimer E., Mikolajewicz U., Hasselmann K. Mean circulation of the Hamburg LSG OGCM and its sensitivity to the thermohaline surface forcing // *J. Phys. Oceanogr.*—1993.—Vol. 23.—P. 731–757.
- [7] Sherbakov A.V., Malakhova V.V. Numerical Modeling of the Ocean Global Climate.—Novosibirsk: IVMiMG, 2008 (In Russian).
- [8] Morales Maqueda M., Holloway G. Second moment advection scheme applied to Arctic ocean simulation // *Ocean Modelling*.—2006.—Vol. 14, No. 3–4.—P. 197–221.—doi:10.1016/j.ocemod.2006.05.003.
- [9] Hecht M.W. Forward-in-time upwind-weighted methods in ocean modeling // *International Journal for Numerical Methods in Fluids*.—2006.—Vol. 50.—P. 1159–1173.
- [10] Golubeva E.N. Numerical modeling of the Atlantic waters dynamics in the Arctic basin using QUICKEST-scheme // *Computer Technologies*.—2008.—Vol. 13, No. 5.—P. 11–24 (In Russian).
- [11] Murray R.J. Explicit generation of orthogonal grids for ocean models // *J. Comput. Phys.*—1996.—Vol. 126.—P. 251–273.
- [12] Kuzin V.I. Finite Element Method in the Oceanic Processes Modeling.—Novosibirsk: VC SO AN SSSR, 1985 (In Russian).
- [13] Golubeva E.N., Ivanov U.A., Kuzin V.I., Platov G.A. Numerical modeling of the World ocean circulation with allowance for the upper quasi-homogeneous layer // *Oceanologia*.—1992.—Vol. 32, Vyp. 3.—P. 395–405 (In Russian).
- [14] Golubeva E.N., Platov G.A. On improving the simulation of Atlantic water circulation in the Arctic ocean // *J. Geophys. Res.*—2007.—Vol. 112, C04S05.—doi:10.1029/2006JC003734.
- [15] Leonard B.P., MacVean M.K., Lock A.P. Positivity-preserving numerical schemes for multidimensional advection.—NASA, March, 1993.—(Technical Memorandum / TM-106055 ICOMP-93-05).
- [16] Prather M.J. Numerical advection by conservation of second-order moments // *J. Geophys. Res.*—1986.—Vol. 91.—P. 6671–6681.
- [17] Steele M., Morley R., Ermold W. PHC: A global hydrography with a high quality Arctic ocean // *J. Climate*.—2000.—Vol. 14, No. 9.—P. 2079–2087.

- [18] Haney R.L. Surface thermal boundary condition for ocean circulation models // *J. Physical Oceanography*. — 1971. — Vol. 1. — P. 241–248.
- [19] Levitus S. Annual cycle of temperature and heat storage in the World Ocean // *J. Phys. Oceanogr.* — 1984. — Vol. 14. — P. 727–746.
- [20] Levitus S. Annual cycle of salinity and salt storage in the World Ocean // *J. Phys. Oceanogr.* — 1984. — Vol. 16. — P. 322–343.
- [21] Trenberth K.E., Olson J.C., Large W.G. A global ocean wind stress climatology based on ECMWF analysis. — Boulder (Colorado): NCAR, 1989. — (NCAR / TN-338+STR).
- [22] Kalnay E., Kanamitsu M., Kistler R., Collins W., Deaven D., et al. The NCEP/NCAR 40-Year Reanalysis Project // *Bull. the American Meteorological Society*. — 1996. — No. 77. — P. 437–471.
- [23] Bryan K., Manabe S., Pacanowsky R.C. Global ocean-atmosphere climate model. Part II. The oceanic circulation // *J. Phys. Oceanogr.* — 1974. — Vol. 5. — P. 30–46.
- [24] Bjerknes J. Atlantic air-sea interaction // *Advances in Geophysics*. — New York: Academic Press, 1964. — Vol. 10. — P. 1–82.
- [25] Leonard B.P. Universal limiter for transient interpolation modeling of the advective transport equations. — NASA, 1988. — (Technical Memorandum / TM-100916 ICOMP-88-11).
- [26] Leonard B.P. The ULTIMATE conservative difference scheme applied to unsteady onedimensional advection // *Computer Methods in Applied Mechanics and Engineering*. — 1991. — Vol. 88. — P. 17–74.